Table V. Geometries Used in the Calculations[a]

	M–C $[a_0]$	M–H $[a_0]$	∠CMH insertion product	∠CMH transition state
Y	4.52	3.77	118°	40°
Zr	4.41	3.64	120°	40°
Nb	4.31	3.50	124°	41°
Mo	4.17	3.30	120°	40°
Tc	4.05	3.15	120°	40°
Ru	3.91	3.02	100°	43°
Rh	3.83	2.80	83°	48°
Pd	3.68	2.87	80°	51°

[a] For each metal the same bond lengths are used for the $HMCH_3$ insertion product and the transition state structure. For the choices of geometries see the discussion in the Appendix.

described by a single reference determinant, the average coupled pair functional (ACPF) method[44] was used. The metal 4d and 5s electrons and all electrons on the CH_4 unit except the C 1s were correlated. In the calculations on the $ClRh(PH_3)_2$ complex all valence electrons on the Cl and PH_3 ligands were also correlated.

The geometry optimizations were performed using slightly smaller basis sets than those described above. On the metal atoms the f-function was deleted, and on carbon the d-function was taken away. The internal methyl structure was kept frozen in all calculations with the C–H bond fixed to 2.082 a_0 and the H–C–H angle to 107.8°. For the molecularly bound methane complex the η^2-structure optimized in ref 25 for the neutral rhodium atom was used for all metals, since the energy is rather insensitive to the exact geometry in this region. The metal–carbon distance used in the η^2-complex is 4.72 au. The geometries for the insertion product and the transition state were partially optimized for most of the metals in the following way. In all cases the metal–carbon and metal–hydrogen distances at the transition state were taken to be the same as for the insertion product. For the palladium system this restriction was found to increase the barrier height by less than 1 kcal/mol (compare ref 24). For yttrium, niobium, and ruthenium the geometries were optimized at the SCF level. The methyl tilt angle was kept at 0° for the $HMCH_3$ insertion product and at 25° for the transition state. Thus, for these metals, the metal–carbon and metal–hydrogen distances, together with the C–M–H angle, were optimized for the insertion product, while for the transition state only the C–M–H angle was optimized. For the rhodium system the geometry of the insertion product was taken from the optimized structure in ref 27. For the transition state of the rhodium system a two-dimensional optimization was performed for the C–M–H bend angle and the methyl tilt angle at both the SCF and the MCPF level. Only the bend angle changed between these two optimizations, and a value of 46° was obtained at the SCF level and 41° at the MCPF level. The energy difference between these two geometries at the MCPF level was only 0.2 kcal/mol, showing that the SCF optimizations should give reliable results. For the palladium system the geometries of the insertion product and the transition state were taken from the optimized structures in ref 22b, with the only modification that the bond distances to the metal in the transition state were taken to be the same as for the insertion product. This modification was made to obtain an equivalent treatment for all the metals. Finally, for zirconium, molybdenum, and technetium the geometries of both the insertion products and the transition states were extrapolated from the above described optimized structures. The geometrical parameters used are summarized in Table V. The errors in relative energies introduced by the nonoptimal geometries are estimated to be on the order of a few kcal/mol.[24,25]

Registry No. Y, 7440-65-5; Zr, 7440-67-7; Nb, 7440-03-1; Mo, 7439-98-7; Tc, 7440-26-8; Ru, 7440-18-8; Rh, 7440-16-6; Pd, 7440-05-3; CH_4, 74-82-8; $HYCH_3$, 141223-15-6; $HZrCH_3$, 141223-16-7; $HNbCH_3$, 141223-17-8; $HMoCH_3$, 141223-18-9; $HTcCH_3$, 141223-19-0; $HRuCH_3$, 141223-20-3; $HRhCH_3$, 141223-21-4; $HPdCH_3$, 93895-87-5.

---

(44) Gdanitz, R. J.; Ahlrichs, R. *Chem. Phys. Lett.* **1988**, *143*, 413.

Transition-Metal Polyhydride Complexes. 3. Relative Stabilities of Classical and Nonclassical Isomers

Zhenyang Lin and Michael B. Hall*

Contribution from the Department of Chemistry, Texas A&M University, College Station, Texas 77843. *Received November 26, 1991*

Abstract: Ab initio calculations with effective core potentials have been used to study the relative stabilities of classical and nonclassical isomers of 18-electron polyhydride transition-metal complexes. Systematic calculations on $ML_{7-n}H_n$ and $ML_{8-n}H_n$ (n = 2–7), where M = Mo, W, Tc, Re, Ru, Os, Rh, and Ir, and L = PH_3 and CO, lead to the following conclusions. The trans influence of two H ligands is significantly destabilizing and influences the stability and structure of the isomers. A diagonal line in the Periodic Table through Ru and Ir divides the classical (left side of the line) and nonclassical (right side of the line) forms for neutral complexes without strong π-accepting ligands. For monocationic hydride complexes the corresponding diagonal line shifts slightly toward early transition metals and crosses between Tc/Ru and Os/Ir. The stability of nonclassical complexes increases with an increase in the number of strong π-accepting ligands or with an increasing contraction of the transition-metal d orbitals. The conclusion for cationic hydride complexes applies to neutral polyhydride transition-metal complexes with a chloride ligand because of the strong electron-withdrawing ability of chloride. Our calculations predict that several complexes previously identified as nonclassical isomers should be reclassified as classical isomers. The trends predicted here also lead to suggestions for finding new classical and nonclassical isomers.

Introduction

Transition-metal polyhydride complexes have been the subject of considerable interest[1-27] since the first discovery of a stable nonclassical dihydrogen complex, $W(CO)_3[P(i\text{-}Pr)_3]_2(\eta^2\text{-}H_2)$, by Kubas et al. It is now clear that polyhydrides may adopt classical

---

(1) (a) Kubas, G. J.; Ryan, R. R.; Swanson, B. J.; Vergamini, P. J.; Wasserman, H. J. *J. Am. Chem. Soc.* **1984**, *106*, 451. (b) Kubas, G. J.; Ryan, R. R.; Wroblewski, D. *J. Am. Chem. Soc.* **1986**, *108*, 1339. (c) Kubas, G. J.; Unkefer, C. J.; Swanson, B. J.; Fukushima, E. *J. Am. Chem. Soc.* **1986**, *108*, 7000. (d) Kubas, G. J. *Acc. Chem. Res.* **1988**, *21*, 120. (e) Khalsa, G. R. K.; Kubas, G. J.; Unkefer, C. J.; van der Sluys, L. S.; Kubat-Martin, K. A. *J. Am. Chem. Soc.* **1990**, *112*, 3855.

(2) (a) Sweany, R. L. *J. Am. Chem. Soc.* **1985**, *107*, 2374. (b) Upmacis, R. K.; Poliakoff, M.; Turner, J. *J. Am. Chem. Soc.* **1986**, *108*, 3645.

(3) (a) Bautista, M. T.; Earl, K. A.; Morris, R. H.; Sella, A. *J. Am. Chem. Soc.* **1987**, *109*, 3780. (b) Bautista, M. T.; Earl, K. A.; Maltby, P. A.; Morris, R. H.; Schweitzer, C. T.; Sella, A. *J. Am. Chem. Soc.* **1987**, *109*, 3780. (c) Earl, K. A.; Polito, M. A.; Morris, R. H. *J. Am. Chem. Soc.* **1987**, *109*, 3780. (d) van der Sluys, L. S.; Eckert, J.; Eisenstein, O.; Hall, J. H.; Huffman, J. C.; Jackson, S. A.; Koetzle, T. F.; Kubas, G. J.; Vergamini, P. J.; Caulton, K. *J. Am. Chem. Soc.* **1990**, *112*, 4831.

0002-7863/92/1514-6102$03.00/0

structures having terminal hydride ligands or nonclassical structures containing η^2-H_2 ligands. Up to now, only a few η^2-H_2 complexes have been unequivocally characterized in the solid state by both X-ray and neutron diffraction techniques,[1,4] while the existence of other η^2-H_2 complexes has been inferred mainly by NMR spectroscopic studies and X-ray crystallographic determinations without locating the positions of hydrogens. In the spectroscopic studies, the ^1H NMR relaxation time T_1 has been used as a criterion to discern classical and nonclassical structures in solutions.[16] Recent studies have revealed that several examples of polyhydrides originally identified as having nonclassical structures according to this criterion, e.g., $ReH_7(dppe)$ and $ReH_5(PPh_3)_3$, are classical polyhydrides.[11,12] More recently, a systematic study of factors that contribute to the relaxation rate (the reciprocal of the relaxation time T_1) of a proton indicated that the original interpretation of T_1 neglected the contributions from dipole–dipole interactions with nuclei other than metal-coordinated protons, which accounted for up to 25% of the observed relaxation rates for nonclassical hydrides and up to 33% for classical complexes in certain cases.[21] It was also shown that for some polyhydrides the observed values of T_1 are consistent with both classical and nonclassical structures. In such cases the T_1 criterion is not able to distinguish between the two possible structures.

Theoretical studies have an opportunity to play a significant role in the interpretation of all these exciting and controversial experimental results. A number of quantum chemical studies on the electronic structure and the relative energies of classical and nonclassical isomers have been restricted to semiempirical methods or to ab initio calculations at the Hartree–Fock (HF) level.[22-26] In a previous paper,[27] we examined the effect of electron correlation and found it to be critical in determining the relative energies of these isomers. Comparing different types of CI calculations, we found that second-order Moller–Plesset (MP2) perturbation calculations[28] provide reliable determination of the relative stability of classical and nonclassical isomers, while configuration interaction with single- and double-excitation (CISD) calculations underestimated the stability of classical hydrides. We also concluded that substitution of PR_3 by PH_3 in most quantum chemical calculations was a reasonable choice.

In this paper, we will examine the factors that contribute to stabilizing one isomer over the other in this class of transition-metal polyhydride complexes by calculating the relative energies of a variety of classical and nonclassical isomers. We also provide some qualitative rules governing the stabilities of classical and nonclassical complexes. Since most known polyhydride complexes contain transition metals in the second and third rows of the Periodic Table and are six-, seven-, or eight-coordinate with a closed-shell configuration of 18 valence electrons, we will focus our discussion on $ML_{7-n}H_n$ and $ML_{8-n}H_n$ (n = 2–7) polyhydride complexes, where M ranges from group 6 to group 8 for second- and third-row transition metals and L can be PH_3 and CO ligands.

Theoretical Details

In this study, all aryl and alkyl groups were replaced by H atoms, i.e., PR_3 was replaced by PH_3. The M–P–H (M is the transition-metal atom) angle was fixed at 115° and the P–H bond distance at 1.44 Å.

Ab initio effective core potentials[29] were employed in all calculations. All geometries were optimized at the restricted Hartree–Fock (HF) level. In certain cases, described in the next section, it was necessary to fix one or more of the H–H distances to produce a model geometry. Except for these cases, the optimized geometries appeared to be local minima because the approximate hessian defined by an update procedure was positive definite. Energies were recalculated with electron correlation included at the MP2 level for all model complexes.

In the effective core potentials (ECPs) for the transition metals, the outermost core orbitals, which correspond to ns^2np^6 configuration, were treated explicitly on an equal footing with the nd, (n+1)s and (n+1)p valence orbitals. The basis sets of the second and third transition series atoms were described with (541/41/211) and (541/41/111), respectively, which correspond to a double-ζ representation of the (n+1)s/np electrons and a triple-ζ representation of the nd electrons. For ligand atoms, the ECPs and double-ζ basis sets of Stevens, Basch, and Krauss were used.[30] [He] and [Ne] configurations were taken as cores for the first- and second-row main group atoms. The Dunning–Huzinaga double-ζ basis set (31) was used for H atoms.[31]

All HF calculations were performed with the GAMESS package[32] while all MP calculations were made by the use of the Gaussian 88 program.[33] All GAMESS calculations were made at the Cornell National Supercomputer Facility (CNSF) on an IBM 3090-600VF, at the Supercomputer Center of Texas A&M University on a Cray Y-MP2/116, or at the

---

(4) (a) Morris, R. H.; Sawyer, J. F.; Shiralian, M.; Zubkowski, J. D. *J. Am. Chem. Soc.* **1985**, *107*, 5581. (b) Ricci, J. S.; Koetzle, T. F.; Bautista, M. T.; Hofstede, T. M.; Morris, R. H.; Sawyer, J. F. *J. Am. Chem. Soc.* **1989**, *111*, 8823. (c) Earl, K. A.; Jia, G.; Maltby, P. A.; Morris, R. H. *J. Am. Chem. Soc.* **1991**, *113*, 3027.

(5) Albertin, G.; Antoniatti, S.; Bordignon, E. *J. Am. Chem. Soc.* **1989**, *111*, 2072.

(6) (a) Chinn, M. S.; Heinekey, D. M.; Payne, N. G.; Sofield, C. D. *Organometallics* **1989**, *8*, 1824. (b) Chinn, M. S.; Heiekey, D. M. *J. Am. Chem. Soc.* **1987**, *109*, 5865.

(7) (a) Hart, D. W.; Bau, R.; Koetzle, T. F. *J. Am. Chem. Soc.* **1977**, *99*, 7557. (b) Wilson, R. D.; Koetzle, T. F.; Hart, D. W.; Kuick, A.; Bau, R. *J. Am. Chem. Soc.* **1977**, *99*, 1775. (c) Suzuki, H.; Lee, D. H.; Oshima, N.; Moro-oka, Y. *Organometallics* **1987**, *6*, 1569. (d) Emge, T. J.; Koetzle, T. F.; Bruno, J. W.; Caulton, K. *Inorg. Chem.* **1984**, *23*, 4012.

(8) Howard, J. A. K.; Johnson, O.; Koetzle, T. F.; Spencer, J. L. *Inorg. Chem.* **1987**, *26*, 2930.

(9) Lyons, D.; Wilkinson, G.; Thornton-Pett, M.; Hursthouse, M. B. *J. Chem. Soc., Dalton Trans.* **1984**, 695.

(10) Gregson, D.; Mason, S. A.; Howard, J. A. K.; Spencer, J. L.; Turner, D. G. *Inorg. Chem.* **1984**, *23*, 4103.

(11) (a) Cotton, F. A.; Luck, R. L. *Inorg. Chem.* **1989**, *28*, 2181. (b) Cotton, F. A.; Luck, R. L. *J. Am. Chem. Soc.* **1989**, *111*, 5757. (c) Cotton, F. A.; Luck, R. L. *J. Chem. Soc., Chem. Commun.* **1988**, 1277.

(12) (a) Howard, J. A. K.; Mason, S. A.; Johnson, O.; Diamond, I. C.; Crennell, S.; Keller, P. A. *J. Chem. Soc., Chem. Commun.* **1988**, 1502. (b) Brammer, L.; Howard, J. A. K.; Johnson, O.; Koetzle, T. F.; Spencer, J. L.; Stinger, A. M. *J. Chem. Soc., Chem. Commun.* **1991**, 241.

(13) (a) Luo, X. L.; Baudry, D.; Boydell, P.; Charpin, P.; Nierlich, M.; Ephritikhine, M.; Crabtree, R. H. *Inorg. Chem.* **1990**, *29*, 1511. (b) Luo, X. L.; Schutle, G. K.; Demoll, P.; Crabtree, R. H. *Inorg. Chem.* **1990**, *29*, 4268.

(14) Luo, X. L.; Crabtree, R. H. *J. Am. Chem. Soc.* **1990**, *112*, 6912.

(15) Garlaschelli, L.; Khan, S. I.; Bau, R.; Longoni, G.; Koetzle, T. F. *J. Am. Chem. Soc.* **1985**, *107*, 7212.

(16) (a) Hamilton, D. G.; Crabtree, R. H. *J. Am. Chem. Soc.* **1988**, *110*, 4126. (b) Crabtree, R. H.; Lavin, M.; Bonneviot, L. *J. Am. Chem. Soc.* **1986**, *108*, 4032. (c) Johnson, T. J.; Huffman, J. C.; Caulton, K. G.; Jackson, S. A.; Eisenstein, O. *Organometallics* **1989**, *8*, 2073.

(17) Mediati, M.; Tachibana, G. N.; Jensen, C. M. *Inorg. Chem.* **1990**, *29*, 5.

(18) (a) Lundquist, E. G.; Huffman, J. C.; Folting, K.; Caulton, K. G. *Angew. Chem., Int. Ed. Engl.* **1988**, *27*, 1165. (b) Lundquist, E. G.; Folting, K.; Streib, W. E.; Huffman, J. C.; Eisenstein, O.; Caulton, K. G. *J. Am. Chem. Soc.* **1990**, *112*, 855.

(19) Jackson, S. A.; Hodges, P. M.; Poliakoff, M.; Turner, J. J.; Grevels, F. W. *J. Am. Chem. Soc.* **1990**, *112*, 1221.

(20) (a) Heinekey, D. M.; Millar, J. M.; Koetzle, T. F.; Payne, N. G.; Zilm, K. W. *J. Am. Chem. Soc.* **1990**, *112*, 909. (b) Zilm, K. W.; Heinekey, D. M.; Millar, J. M.; Payne, G. N.; Neshyba, S. P.; Duchamp, J. C.; Szczyrba, J. *J. Am. Chem. Soc.* **1990**, *112*, 920.

(21) Desrosiers, P. J.; Cai, L.; Lin, Z. R.; Richards, R.; Halpern, J. *J. Am. Chem. Soc.* **1991**, *113*, 4173.

(22) (a) Hay, P. J. *J. Am. Chem. Soc.* **1987**, *109*, 705. (b) Eckart, J.; Kubas, G. J.; Hall, J. H.; Hay, P. J.; Boyle, C. M. *J. Am. Chem. Soc.* **1990**, *112*, 2324.

(23) (a) Saillard, J. Y.; Hoffmann, R. *J. Am. Chem. Soc.* **1984**, *106*, 2006. (b) Burdett, J. K.; Mohammad, R. P. *Organometallics* **1987**, *6*, 1684. (c) Burdett, J. K.; Phillips, J. R.; Mohammad, R. P. *Inorg. Chem.* **1987**, *26*, 3054.

(24) (a) Tsipis, C. A. *Coord. Chem. Rev.* **1991**, *108*, 163. (b) Pacchioni, G. *J. Am. Chem. Soc.* **1990**, *112*, 80.

(25) Maseras, F.; Duran, M.; Lledos, A.; Bertran, J. *J. Am. Chem. Soc.* **1991**, *113*, 2879.

(26) Lin, Z.; Hall, M. B. *Inorg. Chem.* **1991**, *30*, 2569.

(27) Lin, Z.; Hall, M. B. *J. Am. Chem. Soc.* In press.

(28) (a) Moller, C.; Plesset, M. S. *Phys. Rev.* **1936**, *46*, 618. (b) Pople, J. A.; Binkley, J. S.; Seeger, R. *Int. J. Quantum Chem.* **1976**, *S10*, 1.

(29) Hay, P. J.; Wadt, W. R. *J. Chem. Phys.* **1985**, *82*, 299.

(30) Stevens, W. J.; Basch, H.; Krauss, M. *J. Chem. Phys.* **1984**, *81*, 6026.

(31) (a) Huzinaga, S. *J. Chem. Phys.* **1965**, *42*, 1293. (b) Dunning, T. H., Jr. *J. Chem. Phys.* **1970**, *53*, 2823.

(32) Guest, M. F. Daresbury Laboratory, Warrington, WA4 4AD, U.K.

(33) Frisch, M. J.; Head-Gordon, M.; Schlegel, H. B.; Raghavachari, K.; Binkley, J. S.; Gonzalez, C.; Defrees, D. J.; Fox, D. J.; Whiteside, R. A.; Seeger, R.; Melius, C. F.; Baker, J.; Martin, R. L.; Kahn, L. R.; Stewart, J. J. P.; Fluder, E. M.; Topiol, S.; Pople, J. A. *Gaussian 88*; Gaussian, Inc.: Pittsburgh, PA.

Table I. Examples of Polyhydride and Dihydrogen Transition-Metal Complexes

complex[a]	means of structural characterization	geometry of metal ligand core determined or proposed[b]	ref
$M(H)_3(Cp)_2$ (M = Ta, Nb)	X-ray and neutron		7b
$Mo(H)_2(PMe_3)_5$	X-ray and NMR	PB	9
$W(H)_6(PR_3)_3$	X-ray and neutron	TTP	10
$M(C_2H_4)(CO)_3(\eta^2\text{-}H_2)$ (M = Cr, Mo, and W)	IR	octahedral	19
$M(CO)_5(\eta^2\text{-}H_2)$ (M = Cr, Mo, and W)	IR	octahedral	2
$M(CO)_3(PR_3)_2(\eta^2\text{-}H_2)$ (M = Mo and W)	X-ray and neutron for W complex	octahedral	1
$Mo(CO)(dppe)_2(\eta^2\text{-}H_2)$	X-ray and NMR	octahedral	1b
$Re(H)_7(dppe)$	X-ray and neutron	TTP	12a
$Re(H)_7(PR_3)_2$	X-ray and neutron	monocapped SA	12b
$Re(H)_6(SiR_3)(PR_3)_2$	X-ray and NMR	TTP	13a
$Re(H)_2(SiR_3)(CO)(PR_3)_3$	X-ray and NMR	PB	13b
$Re(H)_3(dppe)_2$	X-ray and NMR	PB	3c
$Re(H)_3(PR_3)_4$	X-ray and NMR	PB	11a
$Re(H)_5(PMePh_2)_3$	X-ray and neutron	dodecahedral	7d
$Re(PR_3)_4Cl(\eta^2\text{-}H_2)$	X-ray and NMR	octahedral	11c
$[Re(H)_4(CO)(PR_3)_3]^{+}$[c]	NMR	dodecahedral	14
$[ReCp'(CO)(NO)(\eta^2\text{-}H_2)]^{+}$	NMR	octahedral[d]	6
$Ru(H)_3Cp(PR_3)$	X-ray		7c
$Os(H)_6(PR_3)_2$	X-ray and neutron	dodecahedral	8
$Os(H)_4(PR_3)_3$	X-ray and neutron	PB	7a
$[M(H)(depe)_2(\eta^2\text{-}H_2)]^{+}$ (M = Fe, Ru, and Os)	NMR	octahedral	3
$[Fe(H)(dppe)(\eta^2\text{-}H_2)]^{+}$	X-ray and neutron	octahedral	4
$[RuCp'(CO)_2(\eta^2\text{-}H_2)]^{+}$	NMR	octahedral[d]	6
$[RuCp(dmpe)(\eta^2\text{-}H_2)]^{+}$	NMR	octahedral[d]	6
$[Os(H)_3(PR_3)_3(\eta^2\text{-}H_2)]^{+}$	NMR	PB or octahedral	16a
$Ir(H)_5(PR_3)_2$	X-ray and neutron	PB	15
$[Ir(H)_3(PR_3)Cp]^{+}$	X-ray and neutron		20
$Ir(H)_2(PR_3)_2Cl(\eta^2\text{-}H_2)$	X-ray	octahedral	17
$[Ir(H)(bq)(PR_3)_2(\eta^2\text{-}H_2)]^{+}$	NMR	octahedral	16
$[Ir(H)_2(PR_3)_2(\eta^2\text{-}H_2)_2]^{+}$	NMR	octahedral	16
$[Ir(H)_2(PR_3)_3(\eta^2\text{-}H_2)]^{+}$	NMR	octahedral	18

[a] Cp = $\eta^5\text{-}C_5H_5$, Cp′ = $\eta^5\text{-}C_5Me_5$, dppe = $PPh_2(CH_2)_2PPh_2$, depe = $PEt_2(CH_2)_2PEt_2$, dmpe = $PMe_2(CH_2)_2PMe_2$, bq = 7,8-benzoquinolinate, PB = pentagonal bipyramid, TTP = tricapped trigonal prism, SA = square antiprism. [b] $(\eta^2\text{-}H_2)$ is taken as a single ligand. [c] The co-existence of $[Re(H)_2(CO)(PR_3)(\eta^2\text{-}H_2)]^{+}$ isomer was deduced. [d] Cp (and Cp′) is taken as a tridentate ligand.

Chemistry Department on a FPS Model 522. The Gaussian 88 was run at the CNSF.

Results

A large number of polyhydride transition-metal complexes with classical and nonclassical structures have been synthesized and are summarized in Table I. Throughout this paper, $(\eta^2\text{-}H_2)$ indicates a dihydrogen ligand, $(H)_n$ (n = 1, 2, ...) denotes a classical hydride, and H_n (n = 1, 2, ...) indicates an unspecified structural form. Although the controversial experimental results imply an indefiniteness in the formulae listed in Table I, several trends can be summarized. First, most complexes without strong π-acceptor ligands adopt classical structures, while those with strong π-acceptor ligands prefer nonclassical isomers. Second, for the cationic complexes more nonclassical structures were found. These periodic trends will be examined by using the results of our calculations in the following sections. Starting from both classical and nonclassical isomers for each model complex, we optimized the geometry of each model complex at the HF level. In some cases, both isomers were obtained as local minima, and in other cases, only one isomer was obtained, i.e., results of optimizations led to a single minimum. In the latter case, the H···H separation was fixed at 1.70 Å for the classical isomer and at 0.82 Å for the nonclassical one, and a partial geometry optimization was completed. MP2 calculations were performed to obtain the total energies of these optimized structures.

Table II. Neutral and Cationic Model Complexes without Strong π-Acceptor Ligands and Relative Energies of Classical and Nonclassical Isomers (MP2 Results)

	Neutral Model Complexes		
$MoH_2(PH_3)_5$	$TcH_3(PH_3)_4$	$RuH_4(PH_3)_3$	$RhH_5(PH_3)_2$
−1.1 (**1** → **2**)	5.4 (**3** → **4**)	3.3 (**5** → **6**)	−5.0 (**8** → **9**)
		23.9 (**5** → **7**)	−22.6 (**8** → **10**)
$MoH_4(PH_3)_4$	$TcH_5(PH_3)_3$	$RuH_6(PH_3)_2$	$RhH_7(PH_3)$
18.3 (**13** → **14**)	10.4 (**16** → **17**)	−0.3 (**19** → **20**)	−17.4 (**22** → **23**)
25.9 (**13** → **15**)	20.2 (**16** → **18**)	−6.4 (**19** → **21**)	−38.8 (**22** → **24**)
$WH_2(PH_3)_5$	$ReH_3(PH_3)_4$	$OsH_4(PH_3)_3$	$IrH_5(PH_3)_2$
6.4 (**1** → **2**)	11.5 (**3** → **4**)	13.6 (**5** → **6**)	10.5 (**8** → **9**)
		27.9 (**5** → **7**)	−0.9 (**8** → **10**)
$WH_4(PH_3)_4$	$ReH_5(PH_3)_3$	$OsH_6(PH_3)_2$	$IrH_7(PH_3)$
24.9 (**13** → **14**)	15.2 (**16** → **17**)	5.9 (**19** → **20**)	0.8 (**22** → **23**)
41.0 (**13** → **15**)	31.8 (**16** → **18**)	17.0 (**19** → **21**)	−5.4 (**22** → **24**)
	Cationic Model Complexes		
	$TcH_2(PH_3)_5^{+}$	$RuH_3(PH_3)_4^{+}$	$RhH_4(PH_3)_3^{+}$
	2.0 (**1** → **2**)	−7.2 (**3** → **4**)	−24.8 (**5** → **6**)
$MoH_3(PH_3)_5^{+}$	$TcH_4(PH_3)_4^{+}$	$RuH_5(PH_3)_3^{+}$	$RhH_6(PH_3)_2^{+}$
21.9 (**11** → **12**)	13.9 (**13** → **14**)	−6.8 (**16** → **17**)	−34.3 (**19** → **20**)
	18.9 (**13** → **15**)	−5.8 (**16** → **18**)	−71.2 (**19** → **21**)
	$ReH_2(PH_3)_5^{+}$	$OsH_3(PH_3)_4^{+}$	$IrH_4(PH_3)_3^{+}$
	5.3 (**1** → **2**)	1.9 (**3** → **4**)	−8.2 (**5** → **6**)
$WH_3(PH_3)_5^{+}$	$ReH_4(PH_3)_4^{+}$	$OsH_5(PH_3)_3^{+}$	$IrH_6(PH_3)_2^{+}$
24.1 (**11** → **12**)	17.4 (**13** → **14**)	3.7 (**16** → **17**)	−12.4 (**19** → **20**)
	26.7 (**13** → **15**)	17.7 (**16** → **18**)	−31.7 (**19** → **21**)

For neutral and cationic complexes without strong π-acceptor ligands, we systematically calculated the model complexes listed in Table II. Geometries for these model complexes with different isomers are illustrated in Chart I. In Chart I, the point group of each isomer indicates that symmetry restrictions in the metal–ligand core were imposed in the geometry optimization. Since the $\eta^2\text{-}H_2$ rotation barriers were found to be relatively small,[22] the two H's of the $\eta^2\text{-}H_2$ ligand were always restricted to the same plane as its classical isomer in the geometry optimizations. Partial geometry optimizations were performed for those isomers which could not be found by full geometry optimizations. We fixed a separation of 1.7 Å between the two hydrogens which are involved

Table III. Some Neutral and Cationic Model Complexes with Strong π-Acceptor Ligands and Their Relative Energies of Classical and Nonclassical Isomers (MP2 Results)

	Neutral Model Complexes		
$WH_2(PH_3)_5$	$WH_2(CO)(PH_3)_4$	$WH_2(CO)_2(PH_3)_3$	$WH_2(CO)_3(PH_3)_2$
6.4 (**1** → **2**)	−1.3 (**25** → **26**)	−4.5 (**27** → **28**)	−17.6 (**29** → **30**)
$MoH_4(PH_3)_4$	$MoH_4(CO)(PH_3)_3$		
18.3 (**13** → **14**)	−0.4 (**31** → **32**)		
25.9 (**13** → **15**)	5.9 (**31** → **33**)		
$WH_4(PH_3)_4$	$WH_4(CO)(PH_3)_3$	$WH_4(CO)_4$	
24.9 (**13** → **14**)	8.1 (**31** → **32**)	3.8 (**34** → **35**)	
41.0 (**13** → **15**)	22.6 (**31** → **33**)	−0.3 (**34** → **36**)	
	Cationic Model Complexes		
$TcH_4(PH_3)_4^+$	$TcH_4(CO)(PH_3)_3^+$		
13.9 (**13** → **14**)	−1.8 (**31** → **32**)		
18.9 (**13** → **15**)	2.0 (**31** → **33**)		
$ReH_4(PH_3)_4^+$	$ReH_4(CO)(PH_3)_3^+$		
17.4 (**13** → **14**)	2.0 (**31** → **32**)		
26.7 (**13** → **15**)	9.9 (**31** → **33**)		

in the isomerization to the nonclassical form for the following complexes

$TcH_5(PH_3)_3$ (**16, 17**)
$RuH_6(PH_3)_2$ (**19**)
$RhH_7(PH_3)$ (**22, 23**)
$ReH_2(PH_3)_5^+$ (**1**)
$OsH_3(PH_3)_4^+$ (**3**)
$IrH_7(PH_3)$ (**22, 23**)
$TcH_2(PH_3)_5^+$ (**1**)
$RuH_5(PH_3)_3^+$ (**16, 17**)
$RhH_6(PH_3)_2^+$ (**19, 20**)
$ReH_4(PH_3)_4^+$ (**14**)
$OsH_5(PH_3)_3^+$ (**16**)
$TcH_4(PH_3)_4^+$ (**13, 14**)

and we fixed the η^2-H_2 unit(s) at a separation of 0.82 Å between the two hydrogens which are involved in the isomerization to the classical form for the following complexes

$MoH_4(PH_3)_4$ (**14, 15**)
$WH_4(PH_3)_4$ (**14, 15**)
$ReH_3(PH_3)_4$ (**4**)
$WH_3(PH_3)_5^+$ (**12**)
$ReH_5(PH_3)_5$ (**17, 18**)

The MP2 energy differences between classical and nonclassical isomers for different model complexes are also given in Table II. The energy difference between two isomers is defined as

$$\Delta E = E(\text{nonclassical isomer}) - E(\text{classical isomer})$$

The bold numbers in Table II indicate the isomerizing pair for calculating the energy difference (Chart I). For some model complexes, two ΔE's are presented in Table II. The first one indicates the energy difference between two isomers in column 1 and 2 of Chart I, while the second one denotes the energy difference between two isomers in column 1 and 3 of Chart I. In most cases, the first ΔE is the energy difference between a classical isomer and a nonclassical isomer with one (η^2-H_2) ligand, while the second one is the energy difference between a classical isomer and a nonclassical isomer with two (η^2-H_2) ligands. However, for $RuH_4(PH_3)_3$, $RhH_5(PH_3)_2$, $OsH_4(PH_3)_3$, and $IrH_5(PH_3)_2$ the second ΔE is the energy difference between a classical isomer and a second nonclassical isomer with one (η^2-H_2) ligand (see Chart I). The periodic trends observed in Table II will be discussed later.

For complexes with strong π-accepting ligands, we could make calculations as systematically as the ones above by substituting PH_3 ligands with CO ligands. However, an enormous computational resource would be needed since different numbers of CO's and the site of their substitution would result in a large number of complexes. Therefore, a limited number of model complexes, listed in Table III, was selected to study the most important trends in systems with π-accepting ligands. Geometries for these model complexes are illustrated in Chart II. Partial geometry optimizations were performed for the following isomers

$WH_4(CO)_4$ (**35**)
$TcH_4(CO)(PH_3)_3^+$ (**31, 32**)
$ReH_4(CO)(PH_3)_3^+$ (**32**)

by fixing a separation of 1.7 Å between the two hydrogens which are involved in the isomerization to the nonclassical form, and for the following isomers

$WH_2(CO)(PH_3)_4$ (**26**)
$WH_4(CO)(PH_3)_3$ (**33**)

by fixing the η^2-H_2 unit(s) at a separation of 0.82 Å between the two hydrogens which are involved in the isomerization to the classical form.

Scheme I

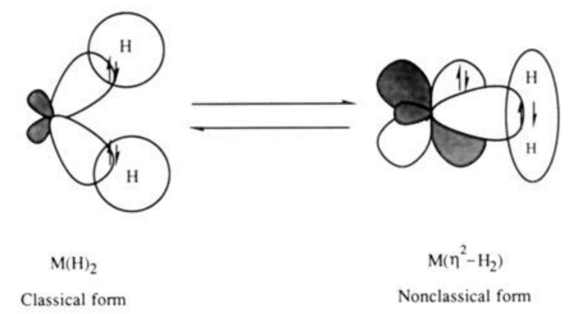

The relative energies, as defined above, of classical and nonclassical carbonyl-containing isomers are given in Table III. The results in Table III show that the stability of nonclassical isomers increases with the number of carbonyls. Again, the trend that the stability of nonclassical isomers increases for cationic complexes is observed by comparing the results of $TcH_4(CO)(PH_3)_3^+$ to $MoH_4(CO)(PH_3)_3$ and $ReH_4(CO)(PH_3)_3^+$ to $WH_4(CO)(PH_3)_3$.

Two chloride model complexes (see Chart III for isomers), $ReH_2Cl(PH_3)_4$ and $IrH_4Cl(PH_3)_2$, were used to calculate the relative energies between classical and nonclassical isomers. For the Re complex, only the classical isomer (**37**) was found to be the local minimum at the HF level, while the nonclassical isomer (**38**) was obtained with partial geometry optimization. All three isomers **39**, **40**, and **41** were local minima at the HF level for the Ir complex. Their relative energies are also given in Chart III. Our results show that the Re complex prefers the classical isomer while the Ir complex adopts the nonclassical one.

Discussion

Before we examine the detailed factors that stabilize one isomer over the other, we provide a bonding scheme (see Scheme I), which was strongly supported by an analysis of the Laplacian of the valence electron density (i.e. $\nabla^2\rho$)[34] on the classical and nonclassical isomers of the $IrH_5(PH_3)_2$ complex in our previous paper.[27] For

---

(34) (a) Bader, R. F. W.; MacDougall, P. J.; Lau, C. D. H. *J. Am. Chem. Soc.* **1984**, *106*, 1594. (b) Bader, R. F. W. *Acc. Chem. Res.* **1985**, *18*, 9.

Chart I

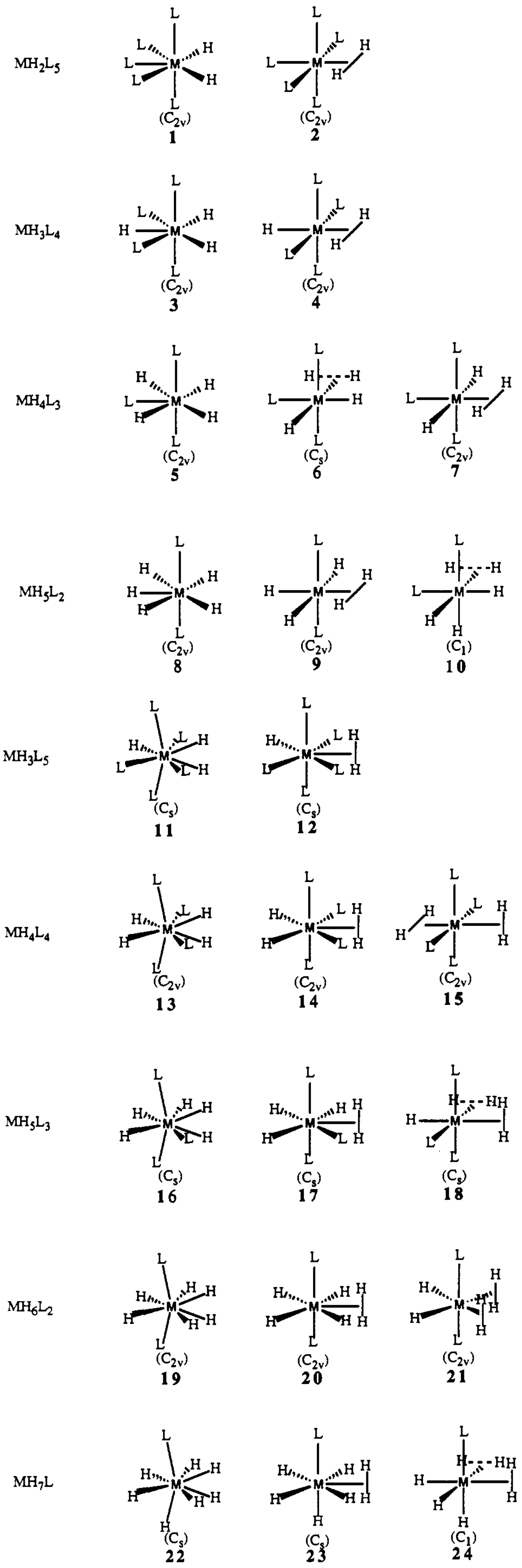

Chart II

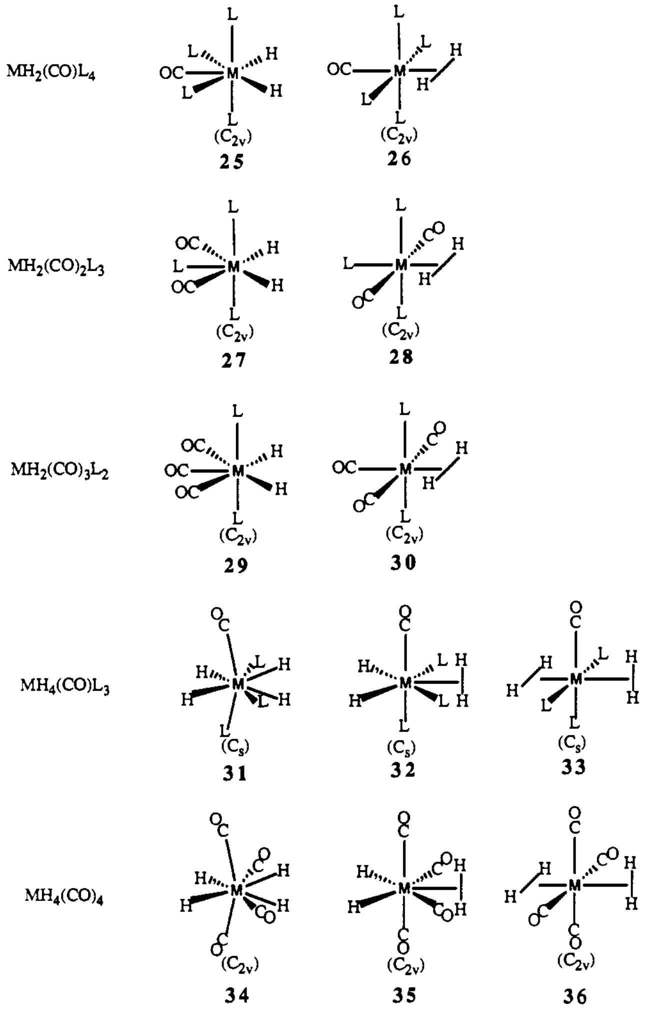

Chart III

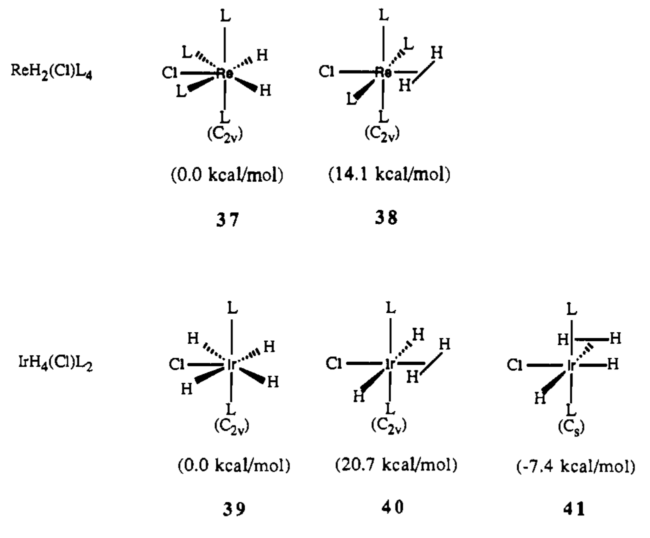

the M(η^2-H_2) nonclassical form, the interaction consists of a primary donation of electron density from the H–H σ bond to an empty metal orbital and a weaker secondary donation of metal d electrons back to the H–H σ^* antibonding orbital.[22,23] For the M$(H)_2$ classical form, the central metal atom formally transfers its d electrons to the hydrides and forms two polar-covalent M–H bonds. The experimental results (see Table I) and our calculations indicate that most complexes adopt classical hydride isomers. This result implies that some special conditions must be met to stabilize nonclassical forms. As we can see from Scheme I, decreasing the tendency of d electron transfer to hydrides would stabilize nonclassical forms. The results presented in the preceding section show that for a hydride complex with strong π-acceptor ligands and/or contracted d orbitals the tendency of d electron transfer decreases and therefore the nonclassical form is more likely.

Trans Influence. In a previous paper,[35] the trans influence[36] was used to predict the relative stabilities of some isomeric hydride complexes. Since H has a strong trans influence, it is particularly significant in the polyhydride complexes when two H ligands are trans to each other. For example, in the model complex $RuH_4(PH_3)_3$, isomer **7** with two H ligands trans to each other is energetically higher by 20.6 kcal/mol than isomer **6** with the two H ligands cis to each other. Likewise, in $OsH_4(PH_3)_3$ isomer **7** is 14.3 kcal/mol higher than isomer **6**. We can also make a comparison between isomers **9** and **10** for model complexes $RhH_5(PH_3)_2$ and $IrH_5(PH_3)_2$. Isomer **9** is 17.6 kcal/mol higher than isomer **10** for the Rh complex and 11.4 kcal/mol higher for the Ir complex (see Table II). For the $IrH_5(PH_3)_2$ complex, we found that isomers **8** and **10** are almost of equal energy (see Table II). Only isomer **8** is found in the crystal structure of $IrH_5[P(i\text{-}Pr)_3]_2$.[15] This result is, most likely, due to the steric effect of two bulky phosphine ligands in isomer **10**. Together, these results show that destabilization of two H ligands trans to each other is significant and should be born in mind when one proposes a structure for a polyhydride complex. No trans pair exists in a dodecahdral geometry and only one occurs along the axial positions in a pentagonal-bipyramidal geometry. The trans influence is particularly important for pseudooctahedral complexes since all ligands are trans to the other.

Neutral and Cationic Complexes without Strong π-Acceptor Ligands. Systematic calculations on this class of metal complexes show that the classical hydrides are preferred for those transition metals with more diffuse d orbitals. The preference of the third row for the classical isomer has its origin in the increasingly diffuse nature of d orbitals on descending the transition-metal group. For transition metals from the same series, the diffuse nature of d orbitals decreases from left to right in the Periodic Table. Therefore, the energy differences between classical and nonclassical isomers decrease from Mo to Rh and W to Ir complexes.

From the periodic trend in the size and vaporization enthalpy of the transition metals, one expects to find a similarity in the diffuse nature of d orbitals along a diagonal line in the Periodic Table. Although the number of calculations is limited, combining the experimental results and our systematic calculations on the eight transition-metal atoms (Mo, Tc, Ru, Rh, W, Re, Os, and Ir), we postulate that a diagonal line divides the transition metals into those that prefer classical forms (left side of the line) and those that prefer nonclassical forms (right side of the line). For those complexes along the diagonal line, both classical and nonclassical isomers may exist. From Table II, we can see that this diagonal line crosses through Ru and Ir for neutral complexes.

For cationic complexes, the corresponding diagonal line shifts toward early transition metals and crosses through between Tc/Ru and Os/Ir metals. This left shift, once again, supports the idea of the diffuse nature of metal d orbitals governing the relative stabilities of classical and nonclassical isomers since increasing the charge on a hydride complex causes its metal d orbitals contract and therefore stabilizes its nonclassical isomer. Indeed, several authors have reported that protonation of neutral classical polyhydride complexes leads to formation of nonclassical isomers.[4,16] For example, $[Ir(H)_2(\eta^2\text{-}H_2)_2(PCy_3)_2]^+$ was obtained through protonation of $IrH_5(PCy_3)_2$ as was $[M(H)(\eta^2\text{-}H_2)(dppe)_2]^+$ (M = Fe, Ru, and Os, and dppe = $PPh_2CH_2CH_2PPh_2$) through protonation of $M(H)_2(dppe)_2$. For the $[OsH_3(PH_3)_4]^+$ complex, our calculations indicate that the classical isomer is slightly more stable by 1.9 kcal/mol (see Table II) than its nonclassical isomer. This small difference explains another report that the related complex $[Os(H\cdots H)(H)(depe)_2]^+$ is a pentagonal-bipyramidal trihydride.[4c]

Calculations predict a slightly more stable nonclassical isomer **2** for $MoH_2(PH_3)_5$. The X-ray crystal structure of $MoH_2(PMe_3)_5$[9] shows a pentagonal-bipyramidal classical geometry with two non-adjacent hydrogens. Calculation based on this X-ray structure still gives a slightly higher energy (1.6 kcal/mol) when compared to isomer **1**. This may be due to the substitution of five PMe_3 by five PH_3 ligands in the model calculations since their substitution slightly overestimates the stability of the nonclassical isomer.[27] We also note that the energy difference between classical and nonclassical isomers for the $WH_2(PH_3)_5$ is smaller than that for $ReH_3(PH_3)_4$, and that for $ReH_3(PH_3)_4$ is smaller than that for $OsH_4(PH_3)_3$ although the former complex in each comparison has more diffuse metal d orbitals than the latter. These two results disagree with the general trend that the energy difference between classical and nonclassical isomers decreases from Mo to Rh and W to Ir complexes (see Table II). Therefore, when earlier transition metals, especially group 6, are compared to later transition metals for neutral complexes with molecular formula MH_nL_{7-n} (L = phosphine), one finds a tendency to stabilize a six-coordinate octahedral structure.

Complexes with Strong π-Acceptor Ligands. The first stable nonclassical complex $W(CO)_3[P(i\text{-}Pr)_3]_2(\eta^2\text{-}H_2)$ synthesized by Kubas et al. has three carbonyls. These carbonyls play a significant role in stabilizing the nonclassical structure. When these carbonyls are substituted by phosphine ligands, the most stable isomer is a classical one (see Tables II and III for $WH_2(PH_3)_5$). As a part of our study of the effect of π-acceptor ligands on the stabilities of classical and nonclassical complexes, we calculated the relative energies of the model complexes $WH_2(CO)_n(PH_3)_{5-n}$ (n = 1, 2, and 3) (see Chart II for structures). The trend that the stabilities of nonclassical isomers increase with the number of carbonyls (see Table III) is strikingly clear although no linear relationship was found. Our calculated energy difference of −17.6 kcal/mol between **29** and **30** for $WH_2(CO)_3(PH_3)_2$ differs substantially from the NMR derived quantity of −1.2 kcal/mol for the $WH_2(CO)_3(P\text{-}i\text{-}Pr_3)_2$ complex.[1e] We do not have an explanation for this discrepancy. The stabilizing effect of carbonyl ligand(s) on nonclassical isomers is also seen in other model calculations (see Table III). To find the relative energies of classical and nonclassical isomers for carbonyl complexes with different transition metals, we used model complexes $MH_4(CO)(PH_3)_3$ (M = Mo, W, Tc^+, Re^+) (see Chart II for structures). The results (see Table III) indicate that both isomers are possible for the Mo complex and the classical isomer is preferred for the W complex. Again, results on $[MH_4(CO)(PH_3)_3]^+$ (M = Tc and Re) show that the most stable isomer is a nonclassical one (**32**) with one (η^2-H_2) ligand for the Tc complex and a classical one (**31**) for the Re complex. Apparently, the more diffuse d orbitals of third-row transition metals are responsible for these observations. Together, these results suggest that the stability of nonclassical complexes depends on the number of π-accepting ligands and the diffuse nature of transition-metal d orbitals. Nonclassical isomers are more likely to be found in complexes with a larger number of π-accepting ligands.

Chloride Complexes. Two chloride complexes,[11c,17] $ReH_2Cl(PMePh_2)_4$ and $IrH_4Cl[P(i\text{-}Pr)_3]_2$, have been synthesized. Spectroscopic (NMR) studies suggested that both complexes adopt nonclassical structures. However, our calculations (see Chart III) give a classical structure for the Re complex and a nonclassical one for the Ir complex. In the optimized classical $Re(H)_2Cl(PH_3)_4$ structure (**37**), the calculated structural parameters for the heavy atoms are very close to the X-ray result.[11c] For example, the calculated Cl–Re–P bond angle in the equatorial plane of the pentagonal-bipyramidal structure is 81.3° while the X-ray result is ca. 83°. Although a nonclassical structure was proposed for the Re complex, it was noted[11c] that the X-ray structural determination at −80 °C was not successful in locating the metal-bonded hydrogen atoms. Our prediction is in agreement with the heavy atom positions, but a final structural determination by neutron diffraction is needed to test the accuracy of our prediction. For the Ir complex, one nonclassical isomer (**40**) is much higher in energy than the other one (**41**). This result is expected because

---

(35) Sargent, A. L.; Hall, M. B. *Inorg. Chem.* **1992**, *31*, 317.

(36) Cotton, F. A.; Wilkinson, G. *Advanced Inorganic Chemistry*, 5th ed.; Wiley: New York, 1988; p 1299.

Scheme II

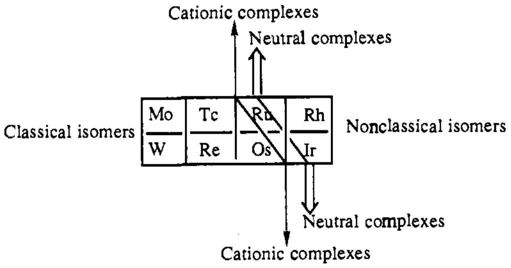

the isomer with two hydrogens trans to each other is disfavored.

The results of our calculations on the two chloride complexes (Re, classical structure; Ir, nonclassical structure) can be understood when one views chloride as a strong electron-withdrawing ligand. The strong electron-withdrawing nature of chloride makes the two complexes cation-like, and therefore, in the Periodic Table, Re is located on the left side of the diagonal line defined above and prefers a classical isomer while Ir is located on the right side of the line and adopts a nonclassical structure.

Conclusion

The stabilities of classical and nonclassical polyhydride transition-metal complexes have been systematically studied. Our calculations predict that ReH$_2$Cl(PMePh$_2$)$_4$[11c] and [OsH$_5$L$_3$]$^+$ (L = PPh$_3$[16a] and PMe$_2$Ph[16c]) should be reclassified as classical isomers. The results of our calculations are presented in Tables II and III. One can use these tables to predict the most stable isomer for those polyhydrides of undetermined structure when these complexes exist and the calculated energy difference is significant. For example, if compounds with molecular formulae RhH$_4$(PR$_3$)$_3$$^+$ and RhH$_6$(PR$_3$)$_2$$^+$ are stable, we can certainly predict the existence of new nonclassical polyhydrides [RhH$_2$(η-H$_2$)(PR$_3$)$_3$]$^+$ (**6**) and [RhH$_2$(η-H$_2$)$_2$(PR$_3$)$_2$]$^+$ (**21**). For those complexes with insignificant energy differences between classical and nonclassical isomers, one predicts that either or both isomers can be adopted.

Since we focus our effort on the periodic trend of the relative stabilities between classical and nonclassical isomers, only selected isomers were discussed. Therefore, we cannot exclude the existence of other isomers which are not investigated. For example, MoH$_2$(PMe$_3$)$_5$ adopts a pentagonal-bipyramidal classical structure with two non-adjacent hydrogens,[9] an isomer not included in this study. Systems that are intermediate between classical and nonclassical isomers, such as ReH$_7${P(C$_6$H$_4$Me)$_3$}$_2$[12b] where neutron diffraction shows a 1.357 Å distance between two hydrogens, are also not considered.

From our systematic calculations, several conclusions have been made. (1) The influence of two H ligands trans to each other is significantly destabilizing. Thus, suggestions of the stability and structure of a polyhydride complex, particularly for those complexes with an octahedral structure, must account for this influence. (2) For neutral complexes without strong π-accepting ligands, a diagonal line in the Periodic Table through Ru and Ir divides the classical (left side of the line) and nonclassical (right side of the line) forms. Those complexes on the line may adopt either or both structures. (3) For monocationic and monochloride hydride complexes, the corresponding diagonal line shifts slightly toward early transition metals and crosses between Tc/Ru and Os/Ir (see Scheme II for illustration of points 2 and 3). (4) The stability of nonclassical complexes with strong π-accepting ligands depends on the number of strong π-accepting ligands and the diffuse nature of the transition-metal d orbitals. The nonclassical isomers are more likely to exist in complexes with a larger number of strong π-accepting ligands.

Acknowledgment. We thank the National Science Foundation (Grant No. CHE 91-13634) and the Robert A. Welch Foundation (Grant No. A-648) for financial support and M. F. Guest for providing the GAMESS package of programs. This research was conducted in part with use of the Cornell National Supercomputer Facility, a resource for the Center for Theory and Simulation in Science and Engineering at Cornell University, which is funded in part by the National Science Foundation, New York State, and the IBM Corp.

Supplementary Material Available: Tables of coordinates of Mo, Tc, Ru, Rh, W, Re, Os, and Ir complexes (38 pages). Ordering information is given on any current masthead page.